

Unsupervised Hashing with Semantic Concept Mining

Rong-Cheng Tu¹²³, Xian-Ling Mao¹²³, Kevin Qinghong Lin⁴, Chengfei Cai⁵, Weize Qin⁶, Hongfa Wang⁶, Wei Wei⁷, Heyan Huang¹²³

¹School of Computer Science and Technology, Beijing Institute of Technology, Beijing, China

²Beijing Engineering Research Center of High Volume Language Information Processing and Cloud Computing Applications, Beijing, China

³Beijing Institute of Technology Southeast Academy of Information Technology, Fujian, China

⁴National University of Singapore, Singapore

⁵School of Computer Science, Zhejiang University, Zhejiang, China

⁶Institute of Computing Technology, Chinese Academy of Sciences, Beijing, China

⁷School of Computer Science, Huazhong University of Science and Technology, Wuhan, China

{tu_rc,maoxl}@bit.edu.cn,linqinghong@email.szu.edu.cn,happyccfnew@163.com,
qinweize@ict.ac.cn,hongfawang@gmail.com,weiw@hust.edu.cn,hhy63@bit.edu.cn

ABSTRACT

Recently, to improve the unsupervised image retrieval performance, plenty of unsupervised hashing methods have been proposed by designing a semantic similarity matrix, which is based on the similarities between image features extracted by a pre-trained CNN model. However, most of these methods tend to ignore high-level abstract semantic concepts contained in images. Intuitively, concepts play an important role in calculating the similarity among images. In real-world scenarios, each image is associated with some concepts, and the similarity between two images will be larger if they share more identical concepts. Inspired by the above intuition, in this work, we propose a novel Unsupervised Hashing with Semantic Concept Mining, called UHSCM, which leverages a VLP model to construct a high-quality similarity matrix. Specifically, a set of randomly chosen concepts is first collected. Then, by employing a vision-language pretraining (VLP) model with the prompt engineering which has shown strong power in visual representation learning, the set of concepts is denoised according to the training images. Next, the proposed method UHSCM applies the VLP model with prompting again to mine the concept distribution of each image and construct a high-quality semantic similarity matrix based on the mined concept distributions. Finally, with the semantic similarity matrix as guiding information, a novel hashing loss with a modified contrastive loss based regularization item is proposed to optimize the hashing network. Extensive experiments on three benchmark datasets show that the proposed method outperforms the state-of-the-art baselines in the image retrieval task. The source codes are available ¹.

¹<https://github.com/rongchentu1/UHSCM>

Permission to make digital or hard copies of all or part of this work for personal or classroom use is granted without fee provided that copies are not made or distributed for profit or commercial advantage and that copies bear this notice and the full citation on the first page. Copyrights for components of this work owned by others than ACM must be honored. Abstracting with credit is permitted. To copy otherwise, or republish, to post on servers or to redistribute to lists, requires prior specific permission and/or a fee. Request permissions from permissions@acm.org.

SIGMOD '23, June 18–23, 2023, SIGMOD, Seattle

© 2022 Association for Computing Machinery.

ACM ISBN 978-1-4503-XXXX-X/18/06... \$15.00

<https://doi.org/10.1145/nnnnnnn.nnnnnnn>

CCS CONCEPTS

• Information systems → Top-k retrieval in databases.

KEYWORDS

Unsupervised Hashing, Image Retrieval, Semantic Concept Mining.

ACM Reference Format:

Rong-Cheng Tu¹²³, Xian-Ling Mao¹²³, Kevin Qinghong Lin⁴, Chengfei Cai⁵, Weize Qin⁶, Hongfa Wang⁶, Wei Wei⁷, Heyan Huang¹²³. 2022. Unsupervised Hashing with Semantic Concept Mining. In *SIGMOD '23: ACM SIGMOD/PODS International Conference on Management of Data, June 18–23, 2023, Seattle, USA*. ACM, 12 pages. <https://doi.org/10.1145/nnnnnnn.nnnnnnn>

1 INTRODUCTION

Recently, with tremendous amounts of image data being generated, image retrieval techniques with fast retrieval speed have attracted much more attention. Among the existing image retrieval techniques, the hashing methods [11, 18, 29, 30, 45, 57, 59, 64] are advantageous due to their high retrieval efficiency and low storage cost. The core idea of image hashing is to map images into compact hash codes while preserving original semantic similarity.

According to whether the training data contains labelling information, existing hashing methods can be roughly divided into two categories: supervised and unsupervised hashing. The supervised ones [7, 27, 33, 38, 49, 53, 55] use the label information of the images to supervise the training of hashing models. Therefore, such methods usually achieve high retrieval performance. Nevertheless, it is time-consuming and expensive to annotate the images. Hence, recently, more and more researchers pay attention to the unsupervised hashing methods [13, 23, 39, 46, 47, 63] which train the hashing models with unlabeled images.

As there is no label information in the unsupervised setting, to improve the retrieval performance, one of the key points is to define a kind of guiding information which sufficiently contains the original similarity of images. Hence, many unsupervised hashing methods focus on defining similarity matrices as guiding information based on the image features extracted usually by a pre-trained CNN model, such as VGG19 [40] or Alexnet [17]. For example, Semantic Structure-based unsupervised Deep Hashing (SSDH) [58]

utilizes the cosine similarity distribution of pairs based on the Gaussian estimation to construct the similarity structure. Furthermore, MLS³RDUH [46] constructs the similarity matrix by utilizing manifold and cosine similarity between image features to reconstruct the local similarity structure.

However, most of these methods define the similarity matrix only depending on the cosine similarity between image features but ignore the high-level abstract semantic concepts contained in the images. Intuitively, the concepts play an important role in calculating the similarity between images. In real-world scenarios, each image is associated with some concepts, and the similarity between two images will be larger if they share more identical concepts. Hence, the semantic concept information is useful to define the similarities between images to further improve the quality of semantic similarity matrix. Moreover, how can the concepts contained in the images be mined? Fortunately, we can leverage vision-language pre-training (VLP) models to mine the concept information contained in the images. By exploiting contrastive learning, these VLP models are directly pre-trained with large-scale noisy image-text pairs which are easily collected from the Internet. With such a broader and cheaper source of data while benefiting from the semantic lever supervision from texts, the VLP models are trained to align the semantic relationships between the images and their corresponding texts. Therefore, by transforming the concepts into texts through a prompt template, the VLP models can be used to align the semantic relationship between images and concept based texts, and then we can obtain the concept information contained in the images.

Therefore, inspired by the above intuition, we propose a novel Unsupervised Hashing with Semantic Concept Mining (UHSCM), which leverages a VLP model CLIP [36] to construct a high-quality similarity matrix through the prompt engineering. Specifically, UHSCM first randomly collects a set of concepts, such as 'cat', 'dog', and 'flower'. Then, by adopting the prompt engineering, UHSCM leverages the CLIP model to denoise the set of randomly collected concepts according to training images. Next, based on the denoised concepts, we utilize the CLIP model with the prompt engineering again to mine the concept distributions of images to construct a high-quality semantic similarity matrix. Finally, incorporating with the semantic similarity matrix as guiding information, a novel hashing loss function with a modified contrastive loss based regularization item is proposed to optimize the hashing network to generate distinguished hash codes. Above all, the main contributions of UHSCM are summarized as follows:

- To the best of our knowledge, the proposed UHSCM is the first work in deep unsupervised hashing, which utilizes a VLP model to mine the concept distributions of images to construct a high-quality semantic similarity matrix.
- A novel contrastive loss based regularization item is proposed for hashing loss to take good use of the constructed semantic similarity matrix to generate distinguished hash codes.
- Extensive experiments on three widely used datasets show that the proposed UHSCM outperforms state-of-the-art unsupervised baselines on image retrieval tasks.

2 RELATED WORK

2.1 Vision-Langue Pre-training Models

Due to the success of BERT [5] in NLP and ViT [6] in computer vision, more and more researchers pay attention to exploring visual-language pre-training (VLP) models [15, 19, 20, 36, 43, 44, 65]. With the contrastive learning, these VLP models are trained to align the semantic relationships between massive image-text pairs which are easily collected from the Internet. Benefiting from such a broader and cheaper source of data, the VLP models have shown strong power in visual representation learning. For example, the recent CLIP [36] and ALIGN [15] employ a contrastive learning strategy on a huge amount of noisy image-text pairs, achieving surprising results on a large number of vision tasks. VATT [1] extends the contrastive learning from the image domain to the video domain and aligns the video frames, audios, and texts. ALBEF [19] proposes a new framework for vision-language representation learning which first aligns the unimodal image representation and text representation before fusing them with a multimodal encoder. Moreover, motivated by CLIP, CoOp [65] further improves the training strategy by proposing a continuous prompting optimization method to achieve better performance on visual classification tasks.

2.2 Image Hashing

Depending on whether supervised information is needed in the training phase, the hashing can be roughly divided into two categories: supervised and unsupervised hashing methods. Please refer to [31, 54] for a comprehensive survey.

Supervised hashing methods [2, 3, 12, 21, 48, 49, 62] learn hash functions by using not only the data representation but also the label information in the training phase. A mass of methods in this category have been proposed, such as Central Similarity Quantization (CSQ) [62] and Partial-Softmax Loss based Deep Hashing (PSLDH) [48]. CSQ first utilizes the Hadamard matrix to generate hash centers for each label, and then pushes the hash codes of images to be close around their hash centers. PSLDH first uses category information with a bit-balance constraint to generate semantic hash codes for each category, and then it leverages the category hash codes as supervision information to guide the learning of the image hashing network by minimizing a Partial-SoftMax loss function.

The unsupervised hashing methods can be divided into traditional unsupervised hashing methods and deep unsupervised hashing methods. The traditional unsupervised hashing methods [10, 26, 28, 29, 56, 61] use hand-crafted features and shallow hash functions to obtain binary hash codes. For example, Anchor Graph Hashing (AGH) [28] proposes a sparse low-rank graph by introducing a set of anchors to speed up the construction of the graph to learn hash codes. Limited by the hand-crafted features and shallow hash functions, it is hard for the traditional shallow hashing methods to generate high-quality hash codes for complex and high dimensional real-world data. Hence, plenty of deep unsupervised hashing methods [22, 24, 32, 46, 47, 58, 60] are recently proposed, which learn deep hashing networks to generate hash codes for images. For example, Semantic structure-based unsupervised deep hashing (SSDH) [58] constructs semantic structures based on a Gaussian estimation to guide hashing network learning. Object

Detection based Deep Unsupervised Hashing (ODDUH) [47] first utilizes an object detection model which is pre-trained on a labeled dataset to obtain the pseudo label information of images, then based on the pseudo label information, it constructs a similarity matrix for the training set to guide the learning of hashing network. MLS³RDUH [46] learns the hashing network by utilizing manifold and cosine similarity between image features to reconstruct the local similarity structure.

Although lots of unsupervised hashing methods have been proposed to improve the quality of similarity matrix of the training set, these constructed matrices are still not good enough because they only depend on the cosine similarity between the image features but ignore the high-level abstract semantic concepts contained in images. Hence, in this paper we propose UHSCM which leverages a VLP model with strong generalization ability to mine the concept information for images to construct a high-quality similarity matrix.

3 PROPOSED METHOD

3.1 Problem Definition

Suppose that a dataset has n images $X = \{\mathbf{x}_i\}_{i=1}^n$, and \mathbf{x}_i denotes the i^{th} image. The goal of unsupervised hashing is to learn a hashing network which maps an image \mathbf{x}_i into a similarity-preserving hash code $\mathbf{b}_i \in \{-1, 1\}^k$ where k is the length of hash codes.

3.2 Design Overview

As shown in Figure 1, UHSCM mainly consists of a semantic similarity generator and a hashing network. In the semantic similarity generator, a VLP model is first used to denoise the set of randomly collected concepts according to the training images. Next, the VLP model is used again to mine the concept distributions of images, and then according to the mined concept distributions, a high-quality semantic similarity matrix of the training set is generated.

Moreover, for the hashing network, it is a VGG19 model with the last layer replaced by a k -dimensional fully-connection layer and $\tanh(\cdot)$ is used as the activation function for the last layer. k is the length of hash codes. In the training phase, with the generated similarity matrix as guiding information, the hashing network will be optimized by a novel hashing loss to map the images $X = \{\mathbf{x}_i\}_{i=1}^n$ into hash codes $Z = \{\mathcal{H}(\mathbf{x}_i; \mathbf{W})\}_{i=1}^n = \{\mathbf{z}_i\}_{i=1}^n \in [-1, 1]^{k \times n}$, where $\mathcal{H} = (\cdot; \mathbf{W})$ denotes the hashing network, and \mathbf{W} is the set of parameters of the hashing network. Then, followed by a $\text{sgn}(\cdot)$ function, the binary hash codes of images can be obtained as $\mathbf{B} = \{\text{sgn}(\mathbf{z}_i)\}_{i=1}^n = \{\mathbf{b}_i\}_{i=1}^n \in \{-1, 1\}^{k \times n}$. $\text{sgn}(\cdot)$ is an element-wise sign function which returns 1 if the input is positive and returns -1 otherwise.

3.3 Semantic Similarity Matrix Generator

3.3.1 Semantic Concept Mining. First, we randomly collect a set of concepts $C = \{\mathbf{c}_i\}_i^m$, where \mathbf{c}_i denotes the i^{th} concept, and m is the total number of concepts. For example, we can directly use the 81 classes defined in NUS-WIDE as the set of concepts. Next, for each concept, we use the following prompt template "a photo of the \mathbf{c}_i " to construct its corresponding text \mathbf{t}_i . Then, for an image \mathbf{x}_i , we use the VLP model to calculate an image-text similarity score

vector $\mathbf{s}_i \in [0, 1]^m$, where the j^{th} item of \mathbf{s}_i denotes the similarity score between \mathbf{x}_i and the j^{th} concept based text \mathbf{t}_j :

$$s_{ij} = \mathcal{F}_{VLP}(\mathbf{x}_i, \mathbf{t}_j; \Theta), \quad (1)$$

where \mathcal{F}_{VLP} denotes the pre-trained VLP model, and Θ is the set of well-learned parameters of the VLP model. Based on the similarity score vector \mathbf{s}_i , the concept distribution of image \mathbf{x}_i can be defined as \mathbf{d}_i :

$$d_{ij} = \frac{e^{\tau s_{ij}}}{\sum_{k=1}^m e^{\tau s_{ik}}}, \quad (2)$$

where τ represents the temperature parameter, and how to set its value will be described in detail in Subsection 4.6; d_{ij} , the j^{th} item of \mathbf{d}_i , denotes the probability of image \mathbf{x}_i containing the j^{th} concept \mathbf{c}_j . The larger value of d_{ij} , the higher probability of image \mathbf{x}_i containing the j^{th} concept \mathbf{c}_j .

Roughly, the semantic similarity a_{ij} between image \mathbf{x}_i and \mathbf{x}_j can be directly calculated by their corresponding concept distributions \mathbf{d}_i and \mathbf{d}_j :

$$a_{ij} = \frac{\mathbf{d}_i^T \mathbf{d}_j}{\|\mathbf{d}_i\|_2 \|\mathbf{d}_j\|_2}, \quad (3)$$

where $\|\cdot\|_2$ denotes l_2 norm.

However, such a way of constructing semantic similarity is not a good choice for the following reason. Since the set of concepts is randomly collected, some of them may not be appropriate for the image dataset, making these concepts useless for distinguishing the images. If we do not eliminate these concepts, they will become noisy and harm the quality of the similarities constructed based on the concept distributions. For example, suppose that a concept \mathbf{c}_i is such a noise that all the images in the dataset do not contain it. But the VLP model may misjudge two dissimilar images both containing the concept \mathbf{c}_i on a high probability, so the two dissimilar images will be mistaken for similar which will misguide the training of the hashing model and harm the retrieval performance. Hence, we propose a way to denoise the set of concepts to make the constructed semantic similarities more high-quality.

3.3.2 Semantic Concept Denoising. With the above calculated concept distributions $\mathbf{D} = \{\mathbf{d}_i\}_{i=1}^n$ of all the images X , then for a concept \mathbf{c}_i , we can calculate its frequency $f(\mathbf{c}_i)$ where it denotes the number of images containing the concept \mathbf{c}_i in the highest probability:

$$f(\mathbf{c}_i) = \sum_{k=1}^n I(j = i | \arg \max_j \mathbf{d}_{kj}), \quad (4)$$

where $I(\cdot)$ is a conditional function which returns 1 when the condition is true otherwise returns 0.

Intuitively, for the concept \mathbf{c}_i , if its frequency f_i is very large or small, i.e., most or only a little bit of images contain it in the highest probability, the concept is a noise, which is useless for distinguishing these images and even will harm the quality of the constructed similarities. Hence, it will be better to discard this concept. Based on that, we define a conditional function to determine whether the concept \mathbf{c}_i needs to be discarded:

$$\text{Discard}(\mathbf{c}_i) = \begin{cases} 0, & \text{if } 0.5 \frac{n}{m} \leq f(\mathbf{c}_i) \leq 0.5n; \\ 1, & \text{otherwise,} \end{cases} \quad (5)$$

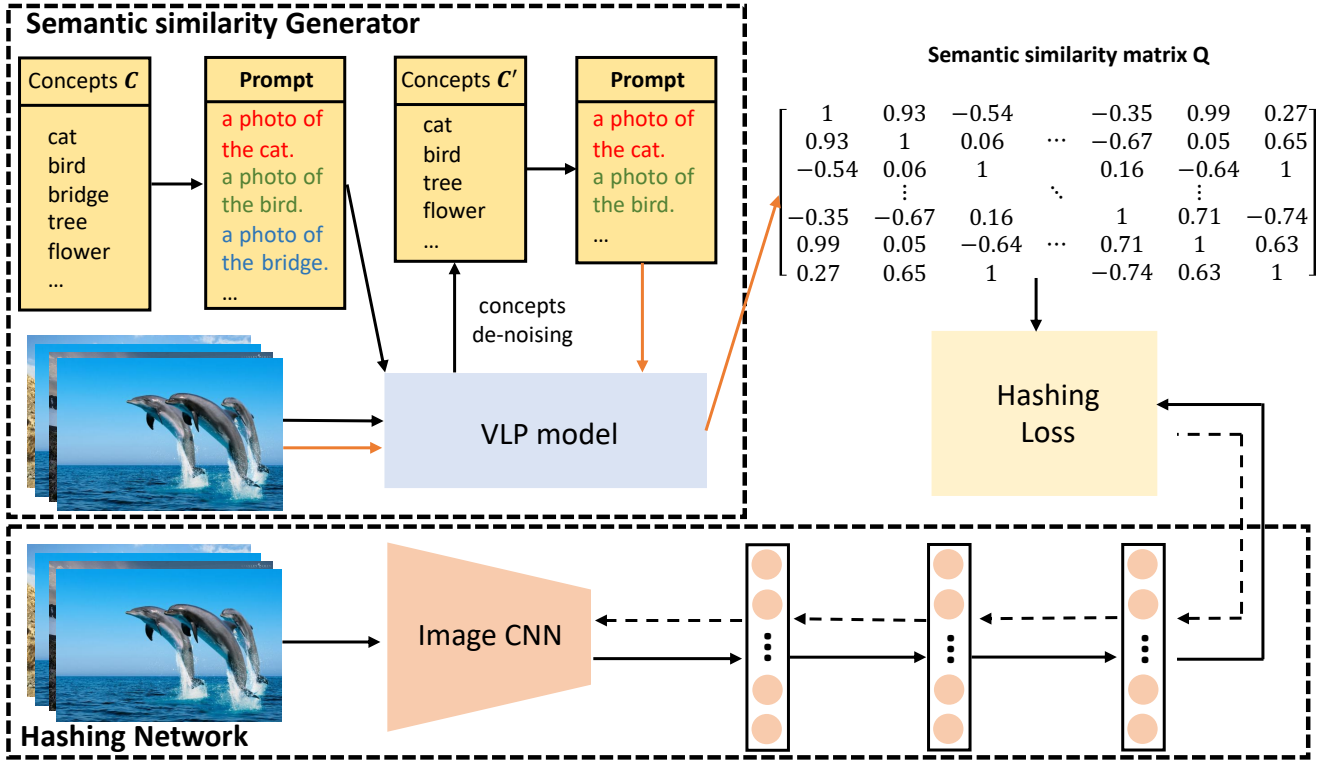


Figure 1: The architecture of UHSCM. The solid arrows indicate forward-propagation, and the dotted arrows indicate back-propagation.

where n is the number of training images, and m is the total number of concepts. When the frequency $f(c_i)$ is larger than $0.5n$, more than half of images contain the concept c_i with the highest probability. It means that more than half of images are defined as similar to each other which will compromise the distinguishability of the generated hash codes; when $f(c_i)$ is smaller than $0.5\frac{n}{m}$, the number of images containing the concept c_i is even smaller than half of the average number of images each concept contained, which is too small then such a concept may not be suitable for this dataset. Hence, in these two cases, the concept c_i should be discarded, i.e., $Discard(c_i) = 1$; in the other cases, i.e., $0.5\frac{n}{m} \leq f(c_i) \leq 0.5n$, it means that the concept may be useful for distinguishing the images, then $Discard(c_i) = 0$.

By keeping the concept c_i whose $Discard(c_i) = 0$ and discarding the one whose $Discard(c_i) = 1$, we can denoise the original set of concepts C to obtain a cleaner concept set $C' = \{c'_i\}_{i=1}^{m'}$, where m' denotes the number of retained useful concepts.

Similar to the calculation of $D = \{d\}_{j=1}^n$, with the set of concepts $C' = \{c'_i\}_{i=1}^{m'}$, we use the VLP model through prompt engineering again to calculate the denoised concept distributions $D' = \{d'\}_{j=1}^n$ for the images X . Finally, we can calculate the high-quality similarity matrix Q :

$$q_{ij} = \frac{d'^T_i d'_j}{\|d'_i\|_2 \|d'_j\|_2}, \quad (6)$$

where q_{ij} is the i^{th} row j^{th} column of Q and denotes the semantic similarity between image x_i and image x_j .

3.4 Learning to Hash

Now, by taking the semantic similarity matrix Q as guiding information, we will train the hashing model to map the images into hash codes with the constructed semantic similarity preserved, i.e., when q_{ij} is so large that image x_i and image x_j are similar, the Hamming distance between their corresponding hash codes b_i and b_j , which is defined as $H_d(b_i, b_j) = \frac{1}{2}(k - b_i^T b_j)$, should be small, otherwise $H_d(b_i, b_j)$ should be large. To achieve this goal, the objective function \mathcal{L} of our hash model is defined as follows:

$$\mathcal{L}_s = \frac{1}{n^2} \sum_{i=1}^n \sum_{j=1}^n (h_{ij} - q_{ij})^2, \quad (7)$$

$$\mathcal{L}_c = \frac{1}{n} \sum_{i=1}^n \sum_{j \in \Psi_i} \frac{1}{|\Psi_i|} \frac{e^{h_{ij}/\gamma}}{e^{h_{ij}/\gamma} + \sum_{l \in \Phi_i} e^{h_{il}/\gamma}}, \quad (8)$$

$$\mathcal{L} = \mathcal{L}_s + \alpha \mathcal{L}_c, \quad (9)$$

where α and γ are the hyper-parameters; h_{ij} denotes the Hamming similarity between the hash codes b_i and b_j which is defined as $h_{ij} = \frac{b_i^T b_j}{\|b_i\|_2 \|b_j\|_2} = \frac{1}{k} b_i^T b_j$. Moreover, $\Psi_i = \{j | q_{ij} \geq \lambda\}$ is the set of indexes of images to which the image x_i should be similar, and λ is

a hyper-parameter. $\Phi_i = \{j | q_{ij} < \lambda\}$ is the set of indexes of images which are not in Ψ_i

Specifically, the first item \mathcal{L}_s is a widely used l_2 loss, which is used to make the learned hash codes preserve the constructed semantic similarity matrix Q well. It can be found that by minimizing the \mathcal{L}_s , when q_{ij} is large, the value of h_{ij} , i.e., $\frac{1}{k} \mathbf{b}_i^T \mathbf{b}_j$ will be large, then the Hamming distance $H_d(\mathbf{b}_i, \mathbf{b}_j)$ will be small; otherwise, $H_d(\mathbf{b}_i, \mathbf{b}_j)$ will be large.

Moreover, the second item \mathcal{L}_c is a modified contrastive loss proposed by us. It can help our hash model further exploit the semantic similarity matrix Q to generate distinguished hash codes. The proposition of \mathcal{L}_c is inspired by the tremendous success of contrastive learning. Although the contrastive loss has been introduced to optimize the hashing model by the CIB [35], it only treats the different views of the same image as similar pairs but does not leverage the constructed semantic similarities to find useful similar data pairs to further improve the retrieval performance. The contrastive loss \mathcal{J}_c defined in the CIB [35] is as follows:

$$\mathcal{J}_c = \frac{1}{n} \sum_{i=1}^n \frac{e^{\text{sim}(\mathbf{b}_i^{(1)}, \mathbf{b}_i^{(2)})/\gamma}}{e^{\text{sim}(\mathbf{b}_i^{(1)}, \mathbf{b}_i^{(2)})/\gamma} + \sum_{l=1, 2} \sum_{k \neq i} e^{e^{\text{sim}(\mathbf{b}_i^{(1)}, \mathbf{b}_k^{(l)})/\gamma}}}, \quad (10)$$

where $\mathbf{b}_i^{(1)}$ and $\mathbf{b}_i^{(2)}$ denote the hash codes of different views of \mathbf{x}_i ; $\text{sim}(\mathbf{b}_i^{(1)}, \mathbf{b}_i^{(2)})$ denotes the Hamming similarity between hash codes. By minimizing the loss \mathcal{J}_c , it just only makes the Hamming similarity between hash codes of different views of the same images higher than that between hash codes of any two different images, no matter whether the two images are similar. It means that the contrastive loss \mathcal{J}_c ignores an amount of useful similarity information between different images. Hence, in our paper, we propose a novel modified contrastive loss \mathcal{L}_c defined as Formula (8). Different from \mathcal{J}_c , without generating different views of images through data augmentation, our modified contrastive loss \mathcal{L}_c directly leverages the semantic similarity matrix Q to construct the similar data pairs. Specifically, in \mathcal{L}_c , when $q_{ij} \geq \lambda$, the image \mathbf{x}_j is treated similar to image \mathbf{x}_i , i.e., the index j belongs to the set Ψ_i of image \mathbf{x}_i . Then, after minimizing \mathcal{L}_c , for each j in Ψ_i , the Hamming similarity between \mathbf{b}_i and \mathbf{b}_j will be larger than that between \mathbf{b}_i and \mathbf{b}_k where $k \notin \Psi_i$. Hence, it makes the generated hash codes more distinguished.

Furthermore, as the each hash code $\mathbf{b}_i = \text{sign}(\mathcal{H}(\mathbf{x}_i; \Theta))$ and the $\text{sign}(\cdot)$ function is in-differentiable at zero and the derivation of it will be zeros for a non-zero input. It means that the parameters of hashing model will not be updated with the back-propagation algorithm when minimizing the loss function \mathcal{L} . Thus, to ensure the parameters of our hashing model are updated, we directly utilize $\tanh(\cdot)$ to approximate the $\text{sign}(\cdot)$ function. Then, similar to previous works [41, 48], we further add a quantization loss to make each element of outputs of the hashing network close to “+1” or

Algorithm 1 Learning algorithm for UHSCM

Input: Images X , the length of hash codes k , a set of randomly selected concepts C .

Output: Parameters of hashing network W , hash codes B .

- 1: Initialize parameters: W , α , β , γ , λ , k , o . learning rate: lr , iteration number: T , mini-batch size t (see Section 4.1).
 - 2: Calculate the concept distributions D of images X over the set of concepts C by the VLP model through prompting.
 - 3: Obtain the clean concept set C' by denoising C with the Formula (4) and Formula (5).
 - 4: Generate the concept distributions D' through the prompt engineering.
 - 5: Calculate the semantic similarity matrix Q .
 - 6: **repeat**
 - 7: **for** $j = 1 : \frac{n}{t}$ **do**
 - 8: Randomly sample t images from database as a mini-batch.
 - 9: Generate hash code \mathbf{z}_i with image \mathbf{x}_i as input by the hash network.
 - 10: Update parameters of the hash network W by minimizing Formula (11).
 - 11: **end for**
 - 12: **until** Convergence
 - 13: Generate binary image hash codes B .
-

“-1”. The final objective function can be formulated as follows:

$$\begin{aligned} \mathcal{L} = & \frac{1}{n^2} \sum_{i=1}^n \sum_{j=1}^n (\hat{h}_{ij} - q_{ij})^2 + \beta \frac{1}{n} \sum_{i=1}^n \|\mathbf{z}_i - \mathbf{b}_i\|_F^2 \\ & + \frac{\alpha}{n} \sum_{i=1}^n \sum_{j \in \Psi_i} \frac{1}{|\Psi_i|} \frac{e^{\hat{h}_{ij}/\gamma}}{e^{\hat{h}_{ij}/\gamma} + \sum_{l \in \Phi_i} e^{\hat{h}_{il}/\gamma}}, \end{aligned} \quad (11)$$

where $\hat{h}_{ij} = \frac{\mathbf{z}_i^T \mathbf{z}_j}{\|\mathbf{z}_i\|_2 \|\mathbf{z}_j\|_2}$; \mathbf{z}_i denotes the hash codes of image \mathbf{x}_i , i.e., the output of hashing network with the input \mathbf{x}_i . The details of the learning procedure are shown in Algorithm 1.

4 EXPERIMENTS

In this section, to evaluate the proposed method UHSCM, extensive experiments are conducted on three commonly used datasets.

4.1 Datasets and Settings

The three datasets used for evaluation are *CIFAR10* [16], *MIRFlickr-25K* [14] and *NUS-WIDE* [4] which are described below.

CIFAR10 is a popular image dataset containing 60,000 images in 10 classes, where each class contains 6,000 images with size 32×32 . We randomly sample 100 images for each class as the test set and use the remaining images as the database, 1,000 images per class from the database as the training set.

NUS-WIDE dataset contains 269,648 images crawled from Flickr. Each image is annotated with one or multiple labels from 81 concept labels. To ensure sufficient samples in each class, only 195,834 images that belong to the 21 most frequent classes are selected for our experiments. Then, we randomly sample 5,000 images as the

Method	CIFAR10				NUS-WIDE				MIRFlickr-25K			
	32 bits	64 bits	96 bits	128 bits	32 bits	64 bits	96 bits	128 bits	32 bits	64 bits	96 bits	128 bits
LSH	0.257	0.286	0.346	0.375	0.538	0.579	0.636	0.666	0.642	0.685	0.701	0.702
SH	0.327	0.339	0.341	0.353	0.612	0.623	0.623	0.626	0.660	0.659	0.654	0.654
ITQ	0.442	0.474	0.479	0.492	0.719	0.743	0.751	0.753	0.763	0.769	0.776	0.776
AGH	0.495	0.491	0.485	0.481	0.727	0.733	0.734	0.732	0.798	0.786	0.777	0.771
SSDH	0.314	0.331	0.352	0.372	0.552	0.596	0.637	0.673	0.749	0.752	0.761	0.762
GH	0.456	0.469	0.500	0.504	0.684	0.720	0.737	0.743	0.744	0.766	0.782	0.791
BGAN	0.583	0.607	0.604	0.612	0.777	0.785	0.790	0.793	0.783	0.793	0.803	0.806
MLS ³ RDUH	0.540	0.550	0.559	0.569	0.776	0.788	0.793	0.796	0.814	0.818	0.817	0.816
CIB	0.580	0.599	0.606	0.611	0.774	0.782	0.782	0.783	0.796	0.808	0.813	0.812
UHSCM	0.831	0.850	0.857	0.853	0.796	0.810	0.813	0.815	0.827	0.834	0.835	0.834

Table 1: MAPs of Hamming ranking for different numbers of hash bits on the three image datasets.

test set and use the remaining images as the database, 10,500 images from the database as the training set.

MIRFlickr-25K contains 25,000 images and each image is labeled with at least one of 24 classes labels. We randomly selected 1,000 images as the test set and the remaining images as the database. In the database, we randomly sample 10,000 images as the training set.

As our proposed method UHSCM is an unsupervised method, we compare it with nine classical and state-of-the-art unsupervised hashing methods: four traditional shallow unsupervised methods LSH [8], SH [56], ITQ [10] and AGH [28]; five deep unsupervised hashing methods: UTH [13], SSDH [58], GH [42], BGAN [41], MLS³RDUH [46], CIB [35]. For fair comparison, we adopt the VGG19 architecture [40] for all the deep hashing methods, and the inputs of the deep hashing methods are the raw images. Moreover, we extract 4,096-dimensional deep features by VGG19 model which is pre-trained on ImageNet [37] dataset as the inputs of the four shallow hashing methods.

In our implementation of UHSCM, we utilize the VGG19 architecture [40] and implement it based on Pytorch framework. We use all the 81 categories of NUS-WIDE directly as the original concepts for all three experimental datasets CIFAR10, NUS-WIDE and MIRFlickr-25k. Note that when conducting the hashing retrieval experiments on the NUS-WIDE dataset, only the images belonging to the 21 most frequent categories are selected. This means that the collected original concepts for the hashing retrieval experiments on the NUS-WIDE dataset still contain many noise concepts. Moreover, the VLP model used in our method is the pre-trained CLIP² model [36]. The parameters in the first eighteen layers of hashing model are initialized with the parameters of the first eighteen layers of VGG19 model which is pre-trained on ImageNet, and the parameters in the nineteen layer of hashing model are initialized by Xavier initialization [9]. We use mini-batch stochastic gradient descent (SGD) with 0.9 momentum and the learning rate is fixed to 0.006. We fix the mini-batch size of images as 128 and the weight decay parameter as 10^{-5} .

4.2 Evaluation Protocol

For hashing based retrieval tasks, Hamming ranking and hash lookup are two widely used retrieval protocols to evaluate the performance of hashing methods [35, 50, 51]. In our experiments, similar to [48], we evaluate the retrieval quality based on three evaluation metrics: Mean Average Precision (**MAP**), Precision curves with respect to the number of top N returned results (**P@n**), Precision-Recall curves (**PR**). MAP, P@n are used to measure the accuracy of the Hamming ranking protocol. PR curve is used to evaluate the accuracy of the hash lookup protocol. Moreover, for the MAP, P@n, and PR curve, the image x_i and image x_j will be defined as a similar pair if x_i and x_j share at least one common label. Otherwise, they will be defined as a dissimilar pair.

Specifically, given a query datapoint, the Average Precision (AP) score of top n retrieved datapoints is defined as:

$$AP = \sum_{i=1}^n \frac{I(i)}{N} \sum_{j=1}^i \frac{I(j)}{i}, \quad (12)$$

where $I(i)$ is an indicator function, if the i^{th} retrieved image is relevant to the query, $I(i) = 1$; otherwise $I(i) = 0$. N represents the number of relevant images in the returned top n datapoints. Then, the Mean Average Precision (MAP) is defined as the average of APs for all queries. Moreover, for all the three datasets, we set n as 5000.

4.3 Experimental Results

4.3.1 Hamming Ranking Protocol. Table 1 shows the MAP results of all baselines and UHSCM on CIFAR10, NUS-WIDE, and MIRFlickr-25K datasets, respectively. The P@N curves on 64 and 128bits over the three datasets are shown in Figure 2. From the table and figures, it can be observed that our method outperforms all state-of-the-art baselines on both the two evaluation metrics. For instance, compared with the latest baseline CIB, the MAP results of our proposed UHSCM have an average increase of 24.8%, 2.8% and 2.5% on datasets CIFAR10, NUS-WIDE and MIRFlickr-25K, respectively. Compared with the best competitor MLS³RDUH on the NUS-WIDE dataset, the MAP results of UHSCM have an average increase of 2.0%. Moreover, as shown in Figure 2, the P@N curves of our method are the highest, and especially the results on CIFAR10 dataset, the

²<https://github.com/openai/CLIP>

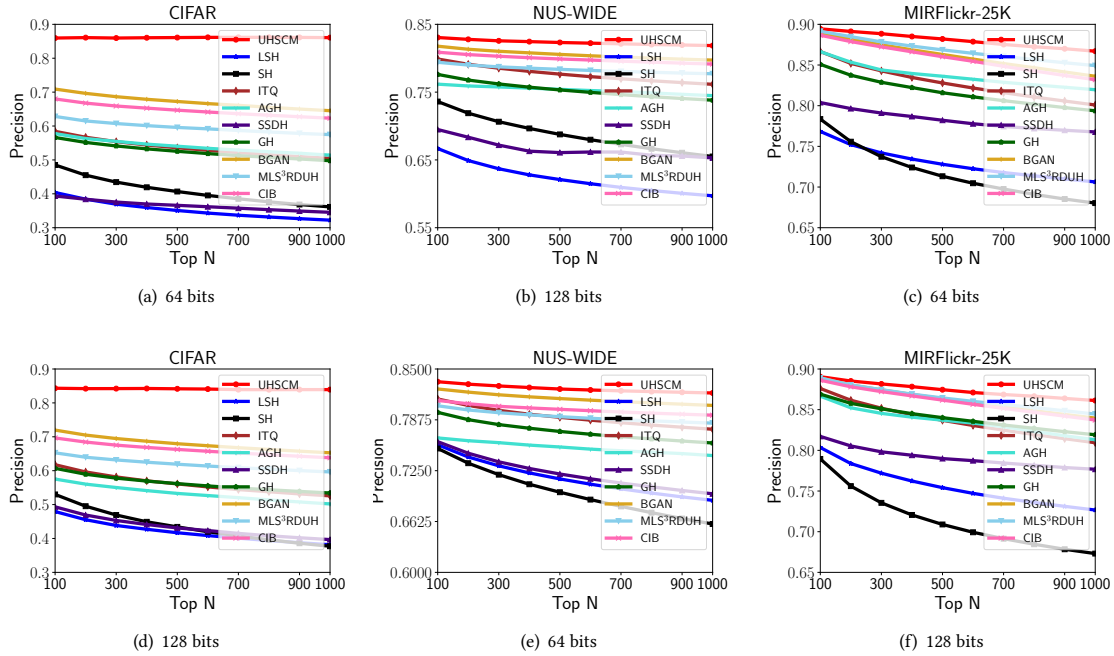


Figure 2: Precision@N curves on the three datasets

Precision@N curves of our proposed UHSCM are greatly larger than all the baselines. These results indicate that the hash codes generated by our proposed method UHSCM can preserve more semantic similarity information than state-of-the-art baselines.

In addition, our proposed UHSCM achieves a large performance improvement on the CIFAR10 dataset compared to the baselines, but the performance improvements on the other two datasets are not as large as on the CIFAR10 dataset. There are two reasons for this: 1) The CIFAR10 is a single-label dataset where it is easy to mine the concept to define high-quality semantic similarity matrix, while the NUS-WIDE and MIRFlickr-25K datasets are multi-label datasets that contain many objects in each image, thus it is difficult to mine the comprehensive and accurate concepts. Therefore, our method can achieve better performance improvement on the CIFAR10 dataset. 2) The performances of existing methods on CIFAR10 are very poor, so it is easy for our method to improve the performance.

4.3.2 Hash Lookup Protocol. When considering the hash lookup protocol, we compute the PR curve for the returned points given any Hamming radius. The PR curve can be obtained by varying the Hamming radius from 0 to k with a step size of 1. The PR curves on 64 and 128bits over the three datasets are shown in Figure 3. It can be found that UHSCM outperforms all the state-of-the-art baselines over all three datasets. For example, as shown in Figure 3 (a) and (d), over the CIFAR10 dataset, the precisions of UHSCM are greatly higher than all the ones of baselines at different recall. Moreover, for the experiments over the NUS-WIDE and MIRFlickr-25K datasets, as shown in Figure 3 (b), (c), (e) and (f), the PR curves of UHSCM are higher than the ones of baselines on the whole. These results demonstrate that the proposed UHSCM can generate hash codes for similar datapoints in a smaller Hamming radius, i.e., the hash

codes generated by the UHSCM are more distinguished than the ones generated by the baselines.

4.4 Ablation Study

To demonstrate the contributions of different components in our proposed model, we conduct several ablation studies on all the three datasets and the results are shown in Table 2. Specifically, the UHSCM in the ‘Ours’ row is the final version used in other experiments. It uses the 81 categories of NUS-WIDE as the original concepts and then uses the semantic concept denoising way proposed in Subsection (3.3.2) to clean up the concepts and generate a semantic similarity matrix, and finally learns the hashing network by minimizing the Formula (11).

4.4.1 Semantic Concept Collection. To investigate the effect of the randomly collected concept set, we design two variants of UHSCM: (1) UHSCM_{coco} uses all 80 categories of MS COCO [25] as the original concepts and with the other setting same as that of UHSCM. (2) UHSCM_{nus&coco} combines all the categories of NUS-WIDE and those of MS COCO and then obtains a total of 153 different categories as the original concepts.

Based on these results shown in ‘1’ and ‘2’ rows of Table 2, it can be observed: (1) Compared with the UHSCM_{coco}, our proposed UHSCM using the 81 categories of NUS-WIDE as the original concepts can achieve better retrieval performance on the NUS-WIDE and MIRFlickr-25K datasets but UHSCM_{coco} performs better on the CIFAR10 dataset. This may be because the 80 categories of MS COCO contain most of the classes of CIFAR10, but are very different with the 21 classes of NUS-WIDE and the 24 classes of MIRFlickr-25K used in our experimental settings. Moreover, the 81 categories of NUS-WIDE contain most of the 21 classes of NUS-WIDE and the 24

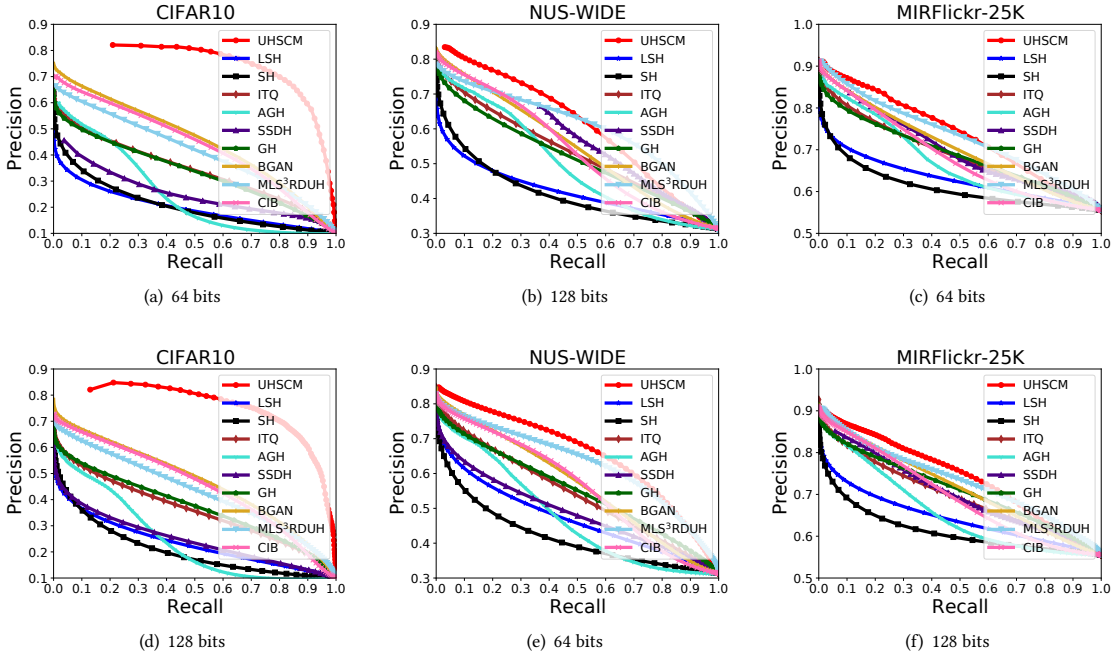


Figure 3: Precision-recall curves on the three datasets

	Method	CIFAR10				NUS-WIDE				MIRFlickr-25K			
		32 bits	64 bits	96 bits	128 bits	32 bits	64 bits	96 bits	128 bits	32 bits	64 bits	96 bits	128 bits
1	UHSCM _{coco}	0.860	0.866	0.863	0.864	0.771	0.785	0.787	0.786	0.801	0.809	0.810	0.812
2	UHSCM _{nus&coco}	0.858	0.865	0.862	0.857	0.789	0.805	0.809	0.810	0.818	0.824	0.825	0.826
3	UHSCM _{IF}	0.761	0.776	0.779	0.763	0.770	0.795	0.803	0.802	0.772	0.792	0.793	0.789
4	UHSCM _{p1}	0.823	0.841	0.843	0.849	0.779	0.798	0.805	0.801	0.801	0.815	0.815	0.814
5	UHSCM _{p2}	0.829	0.846	0.847	0.845	0.770	0.789	0.798	0.803	0.793	0.800	0.799	0.800
6	UHSCM _{avg}	0.834	0.851	0.850	0.857	0.787	0.805	0.803	0.808	0.810	0.824	0.825	0.826
7	UHSCM _{w/o de}	0.791	0.780	0.798	0.791	0.789	0.805	0.809	0.810	0.818	0.827	0.827	0.825
8	UHSCM _{c20}	0.438	0.456	0.469	0.477	0.743	0.764	0.778	0.775	0.769	0.773	0.774	0.777
9	UHSCM _{c30}	0.515	0.543	0.537	0.550	0.753	0.766	0.779	0.789	0.787	0.792	0.797	0.796
10	UHSCM _{c40}	0.601	0.620	0.622	0.637	0.783	0.803	0.806	0.809	0.796	0.798	0.802	0.799
11	UHSCM _{c50}	0.674	0.691	0.685	0.685	0.761	0.781	0.791	0.800	0.810	0.817	0.816	0.815
12	UHSCM _{c60}	0.695	0.697	0.696	0.702	0.771	0.780	0.788	0.792	0.802	0.806	0.807	0.801
13	UHSCM _{w/o MCL}	0.730	0.715	0.700	0.680	0.791	0.801	0.800	0.793	0.813	0.819	0.816	0.814
14	UHSCM _{CL}	0.765	0.800	0.813	0.821	0.783	0.801	0.808	0.810	0.808	0.826	0.830	0.832
Ours	UHSCM	0.831	0.850	0.857	0.853	0.796	0.810	0.813	0.815	0.827	0.834	0.835	0.834

Table 2: MAPs of UHSCM and its variants for different numbers of hash bits on the three image datasets.

classes of MIRFlickr-25K. Hence, UHSCM_{coco} achieves better performance on CIFAR10 dataset and UHSCM performs better on the NUS-WIDE and MIRFlickr-25K datasets. These results show that for two randomly selected concept sets whose number of concepts is almost equal, our proposed method can achieve better retrieval performance when using the concept set with more concepts related to the classes of the experimental dataset as the original concept

set. (2) Comparing the UHSCM_{coco}, UHSCM_{nus&coco} and UHSCM, UHSCM_{coco} achieves the best performance on the CIFAR10 dataset, and UHSCM achieves the best performance on the NUS-WIDE and MIRFlickr-25K datasets. Although the 153 categories collected from MS COCO and NUS-WIDE contain more concepts related to the classes of the three experimental datasets, the UHSCM_{nus&coco} still cannot achieves the best performance on the three datasets. This

may be because the 153 categories contain more useless concepts that confuse the CLIP model and then reduce the quality of the defined semantic similarity matrix. Hence, these results reveal that when lots of useless concepts are contained in the original collected concept set, they will harm the retrieval performance of our hashing model, which also means that it is necessary to denoise the concept set.

4.4.2 Semantic Concept Mining. We design a variant UHSCM_{IF} which directly uses the image features extracted by the CLIP model to construct the semantic similarity matrix without mining the concept semantic distributions through the prompt engineering. As shown in the ‘3’ row of Table 2, compared with the UHSCM_{IF}, the MAP results of UHSCM achieve an average increase of 7.8%, 1.6% and 4.6% on the CIFAR10, NUS-WIDE and MIRFlickr-25K datasets, respectively. It means that the semantic similarity matrix constructed with the concept information is high-quality. These results show that mining the concepts contained in images to construct similarity will improve the retrieval performance of hashing network.

4.4.3 Prompt Template. Here, we study the impact of prompt template. Our proposed UHSCM uses "a photo of the c_i " as the prompt template to construct the corresponding text t_i for c_i , and the UHSCM_{P1} and UHSCM_{P2} use "the c_i " and "it contains the c_i " as the prompt template, respectively. The UHSCM_{avg} is a variant whose semantic similarity matrix is the mean value of the similarity matrices of UHSCM, UHSCM_{P1} and UHSCM_{P2}. As the results shown in the ‘4’ to ‘6’ rows of Table 2, it can be found that using the template "a photo of the c_i " will help our hashing model achieve the best performance. These results show that the prompt template also plays a key role in improving the retrieval performance of our hashing model.

4.4.4 Semantic Concept Denoising. To investigate the effect of our proposed semantic concept denoising component, we propose some variants. First we design a UHSCM_{w/o de} whose semantic similarity matrix is constructed without denoising the set of randomly collected concepts, i.e., calculated by the Formula (3). Next, we define a series of clustering based variants through clustering the original randomly selected concepts into n clusters by K-means [34] and then using the n clusters as the final concepts to generate the semantic similarity matrix, and these variants are termed as UHSCM_{cn} where n denotes the number of clusters. Based on the results shown in the ‘7’ to ‘12’ rows of Table 2, two observations are obtained: (1) The semantic similarity matrix construct with the denoised concepts is more high-quality than that constructed with the randomly collected concepts. For example, compared with the UHSCM_{w/o de}, the MAP results of UHSCM achieve an average increase of 5.8%, 0.5% and 0.8% on the CIFAR10, NUS-WIDE and MIRFlickr-25K datasets, respectively. These results demonstrate that it is necessary to denoise the original randomly selected concept set. (2) Our proposed semantic concept denoising component is more useful than the clustering way. For instance, compared with the best clustering based variant UHSCM_{c50} on MIRFlickr-25K dataset, the MAP results of UHSCM achieve an average increase of 1.8%.

Method	CIFAR10	NUS-WIDE	MIRFlickr-25K
SSDH	24.9	21.2	20.8
GH	25.7	28.4	21.3
BGAN	78.1	83.3	66.1
MLS ³ RDUH	132.7	126.5	114.7
CIB	31.5	34.6	18.5
UHSCM	27.3	35.7	20.2

Table 3: The time consumption (in minute) of our method and baselines on the three image datasets.

4.4.5 Modified Contrastive Loss. To investigate the effect of our proposed modified contrastive loss, we proposed two variants: (1) UHSCM_{w/o MCL} constructs the hashing loss function without the modified contrastive loss \mathcal{L}_c as regularization item; UHSCM_{CL} replace the modified contrastive loss \mathcal{L}_c with the original contrastive loss \mathcal{J}_c to construct the hashing loss function. The corresponding results are shown in the ‘13’ and ‘14’ rows of Table 2. From these results, the following insight can be obtained: (1) With the modified contrastive loss based regularization to optimize the hashing model, it will improve the image retrieval performance. For example, compared with the UHSCM_{w/oMCL}, the MAP results of UHSCM achieve an average increase of 14.4%, 1.2% and 1.7% on the CIFAR10, NUS-WIDE and MIRFlickr-25K datasets, respectively. These results demonstrate that the modified contrastive loss \mathcal{L}_c can further take a good use of the constructed semantic similarity information to guide hashing model generate distinguished hash codes. (2) Our modified contrastive loss \mathcal{L}_c is more useful than the original one \mathcal{J}_c for the hashing model. For example, compared with the UHSCM_{CL}, the MAP results of UHSCM achieve an average increase of 4.8%, 0.8% and 0.9% on the CIFAR10, NUS-WIDE and MIRFlickr-25K datasets, respectively.

4.5 Time Consumption

Here, we investigate the time consumption of our proposed method, and the results are shown in Table 3. In this experiment settings, for a method, its time consumption is the sum of the time spent on all its preprocessing operations and the time spent on training its hashing model to convergence. It can be found that the time consumptions of our proposed method UHSCM are 27.3, 35.7 and 20.2 minutes on the CIFAR10, NUS-WIDE and MIRFlickr-25K datasets, respectively, which are comparable to those of existing methods and even much lower than the ones of BGAN and MLS³RDUH.

4.6 Sensitivity to Hyper-parameters

Here, we investigate the influence of hyper-parameters τ , α , λ , γ , and β with the hash code length being 64 bits on the three datasets.

First, we study the influence of hyper-parameters τ over the three dataset with its value changed from $1m$ to $4m$ and the other hyper-parameters fixed, where m denotes the number of concepts. The MAP results are shown in Figure 4 (a), (f) and (k). It can be found that our proposed method can achieves great retrieval performance on all the three datasets with τ being $1m$ or $3m$. Hence, in the other experiments, we set τ as $3m$.

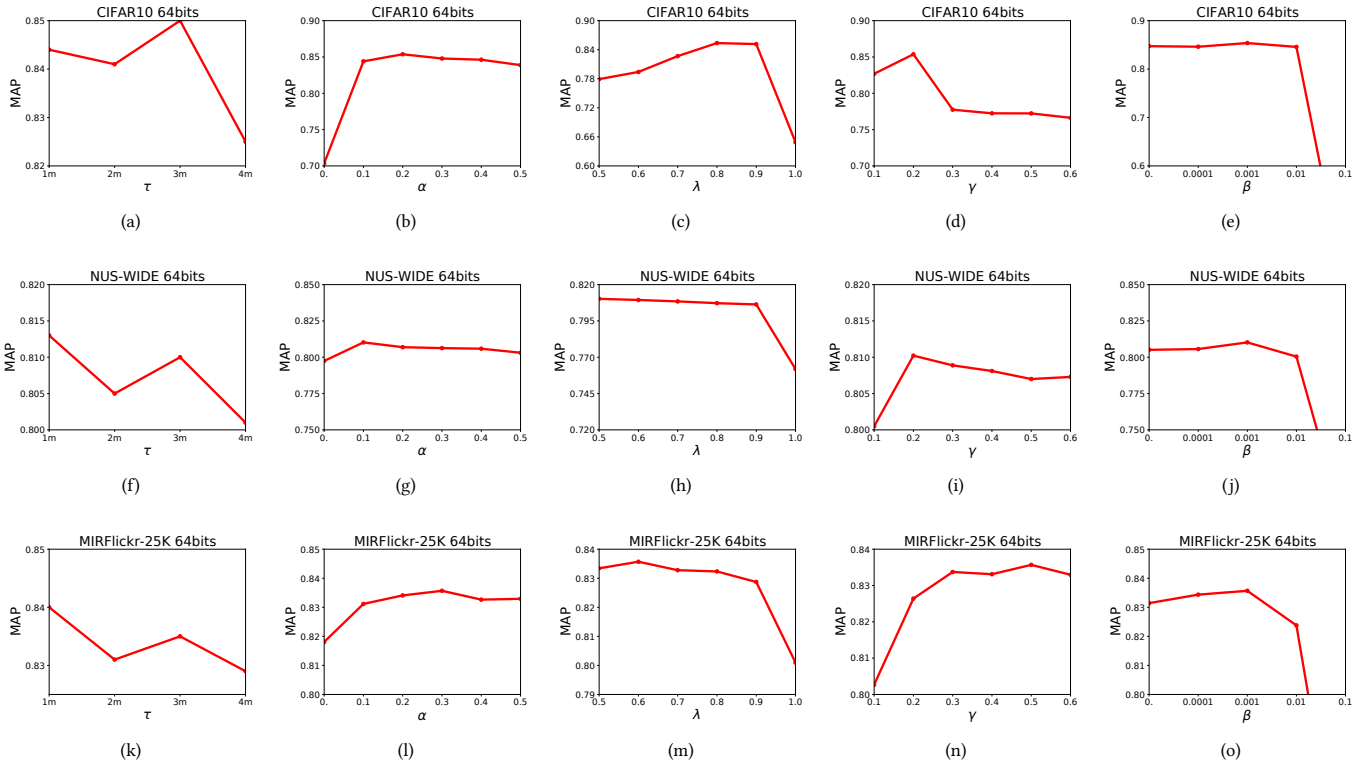


Figure 4: A sensitivity analysis of the hyper-parameters

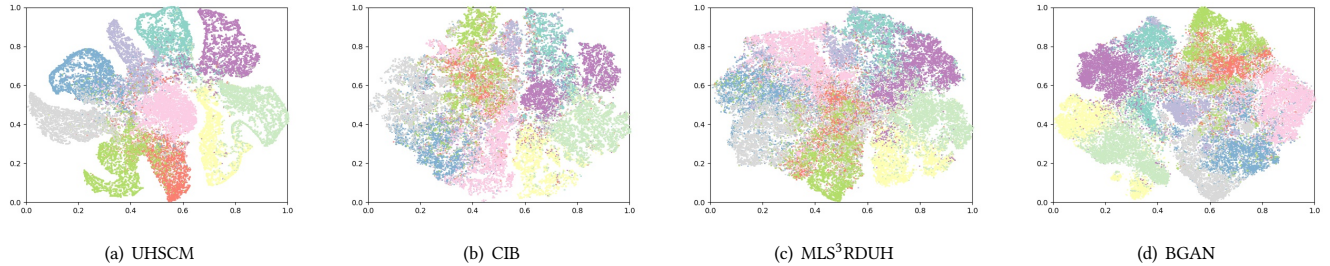


Figure 5: t-SNE visualization on the CIFAR-10 dataset.

Then, to study the influence of hyper-parameter α , we vary the value of α from 0.1 to 0.5 with the other hyper-parameters fixed. As the results shown in Figure 4 (b), (g) and (l) for all the three datasets, UHSCM achieves good performance when $\alpha \in [0.1, 0.4]$. Moreover, for the CIFAR10 dataset, the proposed UHSCM obtains the best retrieval result when $\alpha = 0.2$; for the NUS-WIDE dataset, the performance of UHSCM is the best when $\alpha = 0.1$; for the MIRFlickr-25K dataset, when $\alpha = 0.3$, UHSCM achieves the best retrieval performance.

Next, we investigate the influence of hyper-parameter λ over the three dataset with its value changed from 0.5 to 1.0 and the other hyper-parameters fixed, and the corresponding experimental

results shown in Figure 4 (c), (h) and (m). It can be found that when $\lambda = 0.8, 0.5$ and 0.6 our proposed method UHSCM can achieve the best performance for the CIFAR10, NUS-WIDE and MIRFlickr-25K datasets, respectively.

Moreover, to study the hyper-parameter γ on the three datasets, we vary the value of γ from 0.1 to 0.6 with the other hyper-parameters fixed, and the results are shown in Figure 4 (d), (i) and (n). It can be seen that when $\gamma = 0.2$, our proposed method UHSCM can achieve the best performance for the CIFAR10 and NUS-WIDE datasets, and for the dataset MIRFlickr-25K, UHSCM obtains the best retrieval performance when $\gamma = 0.5$.

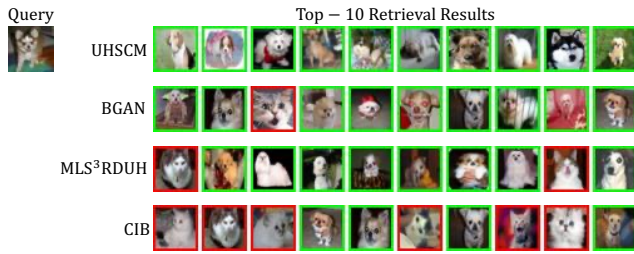


Figure 6: Top-10 retrieved results of UHSCM, CIB, BGAN and MLS³RDUH on the CIFAR-10 dataset.

Furthermore, we investigate the effect of hyper-parameter β with its value varied from 0 to 0.1 and the other hyper-parameters fixed. The MAP results are shown in Figure 4 (d), (h) and (l). For all the three datasets when the $\beta = 0.001$, UHSCM achieves the best performance.

Finally, based on the above experimental results, for the CIFAR10 dataset, we set $\alpha = 0.2$, $\lambda = 0.8$, $\gamma = 0.2$, and $\beta = 0.001$; for the NUS-WIDE dataset, the hyper-parameters α , λ , γ , and β are set as 0.1, 0.5, 0.2 and 0.001, respectively; for the MIRFlickr-25K dataset, we set hyper-parameters α , λ , γ , and β as 0.3, 0.6, 0.5 and 0.001, respectively.

4.7 Qualitative Results

4.7.1 t-SNE visualization. To better understand the manifold structure of learned hashing code, we compare the t-SNE visualization [52] of hash codes generated by our proposed UHSCM, CIB, MLS³RDUH, and BGAN for the datapoints in the database of CIFAR10 dataset, and the results are shown in Figure 5 where the data points within the same colour belong to the same class. It can be easily found that compared with the three baselines, our proposed UHSCM shows a clearer structure, in which the clusters of each class are separated from each other. These results demonstrate that compared with the baselines, our proposed method UHSCM can generate hash codes with more abundant semantic similarity information preserved, i.e., the generated hash codes are more distinguished.

4.7.2 Visualization of retrieval results. In Figure 6, we show the top-10 retrieval results of the proposed UHSCM, CIB, MLS³RDUH and BGAN on the CIFAR-10 dataset with the length of hash codes being 64 bits. Specifically, the relevant results are framed by the green border, and the irrelevant results are framed by the red border. It can be seen that comparing to these baselines, our DSAH has fewer fault images. These results show that the quality of hash codes generated by our proposed UHSCM are higher.

5 CONCLUSION

In this paper, we proposed a novel Unsupervised Hashing with Semantic Concept Mining, dubbed UHSCM. UHSCM first leverages the CLIP model to denoise a set of randomly collected concepts according to the available training images through the prompt engineering. Next, based on the denoised concepts, UHSCM mines the concept distribution of each image by the VLP model through prompting again to constructs a high-quality semantic similarity

matrix. Finally, treating the constructed semantic similarity matrix as guiding information, a novel hashing loss with a modified contrastive loss based regularization item was proposed to optimize the hashing network. Extensive experiments on three benchmark datasets have shown that the proposed method outperforms the state-of-the-art baselines on the image retrieval task.

ACKNOWLEDGMENTS

The work is supported by National Key R&D Plan (No. 2020AAA0106 600), National Natural Science Foundation of China (No. U21B2009, 62172039 and L1924068).

REFERENCES

- [1] Hassan Akbari, Linagzhe Yuan, Rui Qian, Wei-Hong Chuang, Shih-Fu Chang, Yin Cui, and Boqing Gong. 2021. Vatt: Transformers for multimodal self-supervised learning from raw video, audio and text. *arXiv preprint arXiv:2104.11178* (2021).
- [2] Yue Cao, Mingsheng Long, Bin Liu, and Jianmin Wang. 2018. Deep cauchy hashing for hamming space retrieval. In *Proceedings of the IEEE Conference on Computer Vision and Pattern Recognition*. 1229–1237.
- [3] Zhangjie Cao, Mingsheng Long, Jianmin Wang, and Philip S Yu. 2017. Hashnet: Deep learning to hash by continuation. In *Proceedings of the IEEE international conference on computer vision*. 5608–5617.
- [4] Tat-Seng Chua, Jinhui Tang, Richang Hong, Haojie Li, Zhiping Luo, and Yantao Zheng. 2009. NUS-WIDE: a real-world web image database from National University of Singapore. In *Proceedings of the ACM international conference on image and video retrieval*. ACM, 48.
- [5] Jacob Devlin, Ming-Wei Chang, Kenton Lee, and Kristina Toutanova. 2018. Bert: Pre-training of deep bidirectional transformers for language understanding. *arXiv preprint arXiv:1810.04805* (2018).
- [6] Alexey Dosovitskiy, Lucas Beyer, Alexander Kolesnikov, Dirk Weissenborn, Xi-aohua Zhai, Thomas Unterthiner, Mostafa Dehghani, Matthias Minderer, Georg Heigold, Sylvain Gelly, et al. 2020. An image is worth 16x16 words: Transformers for image recognition at scale. *arXiv preprint arXiv:2010.11929* (2020).
- [7] Sepelr Eghbali and Ladan Tahvildari. 2019. Deep Spherical Quantization for Image Search. In *Proceedings of the IEEE Conference on Computer Vision and Pattern Recognition*. 11690–11699.
- [8] Aristides Gionis, Piotr Indyk, Rajeev Motwani, et al. 1999. Similarity search in high dimensions via hashing. In *Vldb*, Vol. 99. 518–529.
- [9] Xavier Glorot and Yoshua Bengio. 2010. Understanding the difficulty of training deep feedforward neural networks. In *Proceedings of the thirteenth international conference on artificial intelligence and statistics*. 249–256.
- [10] Yunchao Gong, Svetlana Lazebnik, Albert Gordo, and Florent Perronnin. 2012. Iterative quantization: A procrustean approach to learning binary codes for large-scale image retrieval. *IEEE Transactions on Pattern Analysis and Machine Intelligence* 35, 12 (2012), 2916–2929.
- [11] Junfeng He, Wei Liu, and Shih-Fu Chang. 2010. Scalable similarity search with optimized kernel hashing. In *Proceedings of the 16th ACM SIGKDD international conference on Knowledge discovery and data mining*. 1129–1138.
- [12] Long-Kai Huang, Jianda Chen, and Sinno Jialin Pan. 2019. Accelerate Learning of Deep Hashing With Gradient Attention. In *Proceedings of the IEEE International Conference on Computer Vision*. 5271–5280.
- [13] Shanshan Huang, Yichao Xiong, Ya Zhang, and Jia Wang. 2017. Unsupervised Triplet Hashing for Fast Image Retrieval. In *Proceedings of the on Thematic Workshops of ACM Multimedia 2017*. ACM, 84–92.
- [14] Mark J Huiskes and Michael S Lew. 2008. The mir flickr retrieval evaluation. In *Proceedings of the 1st ACM international conference on Multimedia information retrieval*. 39–43.
- [15] Chao Jia, Yinfei Yang, Ye Xia, Yi-Ting Chen, Zarana Parekh, Hieu Pham, Quoc V Le, Yunhsuan Sung, Zhen Li, and Tom Duerig. 2021. Scaling up visual and vision-language representation learning with noisy text supervision. *arXiv preprint arXiv:2102.05918* (2021).
- [16] Alex Krizhevsky, Geoffrey Hinton, et al. 2009. *Learning multiple layers of features from tiny images*. Technical Report. Citeseer.
- [17] Alex Krizhevsky, Ilya Sutskever, and Geoffrey E Hinton. 2012. Imagenet classification with deep convolutional neural networks. *Advances in neural information processing systems* 25 (2012), 1097–1105.
- [18] Chao Li, Cheng Deng, Ning Li, Wei Liu, Xinbo Gao, and Dacheng Tao. 2018. Self-supervised adversarial hashing networks for cross-modal retrieval. In *Proceedings of the IEEE conference on computer vision and pattern recognition*. 4242–4251.
- [19] Junnan Li, Ramprasaath Selvaraju, Akhilesh Gotmare, Shafiq Joty, Caiming Xiong, and Steven Chu Hong Hoi. 2021. Align before fuse: Vision and language representation learning with momentum distillation. *Advances in Neural Information Processing Systems* 34 (2021).

- [20] Liunian Harold Li, Mark Yatskar, Da Yin, Cho-Jui Hsieh, and Kai-Wei Chang. 2019. Visualbert: A simple and performing baseline for vision and language. *arXiv preprint arXiv:1908.03557* (2019).
- [21] Wu-Jun Li, Sheng Wang, and Wang-Cheng Kang. 2016. Feature learning based deep supervised hashing with pairwise labels. In *Proceedings of the Twenty-Fifth International Joint Conference on Artificial Intelligence*. AAAI Press, 1711–1717.
- [22] Kevin Lin, Jiwen Lu, Chu-Song Chen, and Jie Zhou. 2016. Learning compact binary descriptors with unsupervised deep neural networks. In *Proceedings of the IEEE Conference on Computer Vision and Pattern Recognition*. 1183–1192.
- [23] Qinghong Lin, Xiaojun Chen, Qin Zhang, Shangxuan Tian, and Yudong Chen. 2021. Deep Self-Adaptive Hashing for Image Retrieval. In *Proceedings of the 30th ACM International Conference on Information & Knowledge Management*. 1028–1037.
- [24] Qinghong Lin, Xiaojun Chen, Qin Zhang, Shangxuan Tian, and Yudong Chen. 2021. Deep Self-Adaptive Hashing for Image Retrieval. In *Proceedings of the 30th ACM International Conference on Information & Knowledge Management*. 1028–1037.
- [25] Tsung-Yi Lin, Michael Maire, Serge Belongie, James Hays, Pietro Perona, Deva Ramanan, Piotr Dollár, and C Lawrence Zitnick. 2014. Microsoft coco: Common objects in context. In *European Conference on Computer Vision*. Springer, 740–755.
- [26] Wei Liu, Cun Mu, Sanjiv Kumar, and Shih-Fu Chang. 2014. Discrete graph hashing. *Advances in neural information processing systems* 27 (2014).
- [27] Wei Liu, Jun Wang, Rongrong Ji, Yu-Gang Jiang, and Shih-Fu Chang. 2012. Supervised hashing with kernels. In *2012 IEEE conference on computer vision and pattern recognition*. IEEE, 2074–2081.
- [28] Wei Liu, Jun Wang, Sanjiv Kumar, and Shih-Fu Chang. 2011. Hashing with graphs. In *icml*.
- [29] Wei Liu, Jun Wang, Yadong Mu, Sanjiv Kumar, and Shih-Fu Chang. 2012. Compact hyperplane hashing with bilinear functions. *arXiv preprint arXiv:1206.4618* (2012).
- [30] Wei Liu and Tongtao Zhang. 2016. Multimedia hashing and networking. *IEEE MultiMedia* 23, 3 (2016), 75–79.
- [31] Xiao Luo, Haixin Wang, Daqing Wu, Chong Chen, Minghua Deng, Jianqiang Huang, and Xian-Sheng Hua. 2020. A survey on deep hashing methods. *ACM Transactions on Knowledge Discovery from Data (TKDD)* (2020).
- [32] Xiao Luo, Daqing Wu, Zeyu Ma, Chong Chen, Minghua Deng, Jinwen Ma, Zhongming Jin, Jianqiang Huang, and Xian-Sheng Hua. 2020. Cimon: Towards high-quality hash codes. *arXiv preprint arXiv:2010.07804* (2020).
- [33] Xin Luo, P. Zhang, Zi Huang, L. Nie, and Xin-Shun Xu. 2019. Discrete Hashing With Multiple Supervision. *IEEE Transactions on Image Processing* 28 (2019), 2962–2975.
- [34] J MacQueen. 1967. Classification and analysis of multivariate observations. In *5th Berkeley Symp. Math. Statist. Probability*. 281–297.
- [35] Zexuan Qiu, Qinliang Su, Zijing Ou, Jianxing Yu, and Changyou Chen. 2020. Unsupervised Hashing with Contrastive Information Bottleneck. In *IJCAI*.
- [36] Alec Radford, Jong Wook Kim, Chris Hallacy, Aditya Ramesh, Gabriel Goh, Sandhini Agarwal, Girish Sastry, Amanda Askell, Pamela Mishkin, Jack Clark, et al. 2021. Learning transferable visual models from natural language supervision. *arXiv preprint arXiv:2103.00020* (2021).
- [37] Olga Russakovsky, Jia Deng, Hao Su, Jonathan Krause, Sanjeev Satheesh, Sean Ma, Zhiheng Huang, Andrej Karpathy, Aditya Khosla, Michael Bernstein, et al. 2015. Imagenet large scale visual recognition challenge. *International journal of computer vision* 115, 3 (2015), 211–252.
- [38] Fumin Shen, Chunhua Shen, Wei Liu, and Heng Tao Shen. 2015. Supervised discrete hashing. In *Proceedings of the IEEE conference on computer vision and pattern recognition*. 37–45.
- [39] Yuming Shen, Jie Qin, Jiabin Chen, Mengyang Yu, Li Liu, Fan Zhu, Fumin Shen, and Ling Shao. 2020. Auto-Encoding Twin-Bottleneck Hashing. In *Proceedings of the IEEE/CVF Conference on Computer Vision and Pattern Recognition*. 2818–2827.
- [40] Karen Simonyan and Andrew Zisserman. 2014. Very deep convolutional networks for large-scale image recognition. *arXiv preprint arXiv:1409.1556* (2014).
- [41] Jingkuan Song, Tao He, Lianli Gao, Xing Xu, Alan Hanjalic, and Heng Tao Shen. 2018. Binary generative adversarial networks for image retrieval. In *Thirty-second AAAI conference on artificial intelligence*.
- [42] Shupeng Su, Chao Zhang, Kai Han, and Yonghong Tian. 2018. Greedy hash: Towards fast optimization for accurate hash coding in cnn. In *Proceedings of the 32nd International Conference on Neural Information Processing Systems*. 806–815.
- [43] Weijie Su, Xizhou Zhu, Yue Cao, Bin Li, Lewei Lu, Furu Wei, and Jifeng Dai. 2019. Vi-bert: Pre-training of generic visual-linguistic representations. *arXiv preprint arXiv:1908.08530* (2019).
- [44] Hao Tan and Mohit Bansal. 2019. Lxmert: Learning cross-modality encoder representations from transformers. *arXiv preprint arXiv:1908.07490* (2019).
- [45] Rong-Cheng Tu, Lei Ji, Huaishao Luo, Botian Shi, He-Yan Huang, Nan Duan, and Xian-Ling Mao. 2021. Hashing based Efficient Inference for Image-Text Matching. In *Findings of the Association for Computational Linguistics: ACL-IJCNLP 2021*. 743–752.
- [46] Rong-Cheng Tu, Xianling Mao, and Wei Wei. 2020. MLS3RDUH: Deep Unsupervised Hashing via Manifold based Local Semantic Similarity Structure Reconstructing. In *IJCAI*. 3466–3472.
- [47] Rong-Cheng Tu, Xian-Ling Mao, Bo-Si Feng, and Yu Shu-Ying. 2018. Object detection based deep unsupervised hashing. In *IJCAI*. 3606–3612.
- [48] Rong-Cheng Tu, Xian-Ling Mao, Jia-Nan Guo, Wei Wei, and Heyan Huang. 2021. Partial-Softmax Loss based Deep Hashing. In *Proceedings of the Web Conference 2021*. 2869–2878.
- [49] Rong-Cheng Tu, Xian-Ling Mao, Cihang Kong, Zihang Shao, Ze-Lin Li, Wei Wei, and Heyan Huang. 2021. Weighted Gaussian Loss based Hamming Hashing. In *Proceedings of the 29th ACM International Conference on Multimedia*. 3409–3417.
- [50] Rong-Cheng Tu, Xian-Ling Mao, Bing Ma, Yong Hu, Tan Yan, Wei Wei, and Heyan Huang. 2020. Deep cross-modal hashing with hashing functions and unified hash codes jointly learning. *IEEE Transactions on Knowledge and Data Engineering* (2020).
- [51] Rong-Cheng Tu, Xian-Ling Mao, Rong-Xin Tu, Binbin Bian, Chengfei Cai, Wei Wei, Heyan Huang, et al. 2022. Deep cross-modal proxy hashing. *IEEE Transactions on Knowledge and Data Engineering* (2022).
- [52] Laurens Van der Maaten and Geoffrey Hinton. 2008. Visualizing data using t-SNE. *Journal of machine learning research* 9, 11 (2008).
- [53] Dan Wang, Heyan Huang, Chi Lu, Bo-Si Feng, Liqiang Nie, Guihua Wen, and Xian-Ling Mao. 2017. Supervised deep hashing for hierarchical labeled data. *arXiv preprint arXiv:1704.02088* (2017).
- [54] Jun Wang, Wei Liu, Sanjiv Kumar, and Shih-Fu Chang. 2015. Learning to hash for indexing big data—A survey. *Proc. IEEE* 104, 1 (2015), 34–57.
- [55] Jun Wang, Wei Liu, Andy X Sun, and Yu-Gang Jiang. 2013. Learning hash codes with listwise supervision. In *Proceedings of the IEEE international conference on computer vision*. 3032–3039.
- [56] Yair Weiss, Antonio Torralba, and Rob Fergus. 2009. Spectral hashing. In *Advances in neural information processing systems*. 1753–1760.
- [57] Erkun Yang, Cheng Deng, Chao Li, Wei Liu, Jie Li, and Dacheng Tao. 2018. Shared predictive cross-modal deep quantization. *IEEE transactions on neural networks and learning systems* 29, 11 (2018), 5292–5303.
- [58] Erkun Yang, Cheng Deng, Tongliang Liu, Wei Liu, and Dacheng Tao. 2018. Semantic structure-based unsupervised deep hashing. In *Proceedings of the 27th International Joint Conference on Artificial Intelligence*. 1064–1070.
- [59] Erkun Yang, Cheng Deng, Wei Liu, Xianglong Liu, Dacheng Tao, and Xinbo Gao. 2017. Pairwise relationship guided deep hashing for cross-modal retrieval. In *proceedings of the AAAI Conference on Artificial Intelligence*, Vol. 31.
- [60] Erkun Yang, Tongliang Liu, Cheng Deng, Wei Liu, and Dacheng Tao. 2019. DistillHash: Unsupervised Deep Hashing by Distilling Data Pairs. In *Proceedings of the IEEE Conference on Computer Vision and Pattern Recognition*. 2946–2955.
- [61] Felix Yu, Sanjiv Kumar, Yunchao Gong, and Shih-Fu Chang. 2014. Circulant binary embedding. In *International conference on machine learning*. 946–954.
- [62] Li Yuan, Tao Wang, Xiaopeng Zhang, Francis EH Tay, Zequn Jie, Wei Liu, and Jiashi Feng. 2020. Central similarity quantization for efficient image and video retrieval. In *Proceedings of the IEEE/CVF Conference on Computer Vision and Pattern Recognition*. 3083–3092.
- [63] Kun Zhan, J. Guan, Yi Yang, and Qun Wu. 2016. Unsupervised discriminative hashing. *J. Vis. Commun. Image Represent.* 40 (2016), 847–851.
- [64] Hanwang Zhang, Fumin Shen, Wei Liu, Xiangnan He, Huanbo Luan, and Tat-Seng Chua. 2016. Discrete collaborative filtering. In *Proceedings of the 39th International ACM SIGIR conference on Research and Development in Information Retrieval*. 325–334.
- [65] Kaiyang Zhou, Jingkang Yang, Chen Change Loy, and Ziwei Liu. 2021. Learning to prompt for vision-language models. *arXiv preprint arXiv:2109.01134* (2021).